Rev. Adv. Mater. Sci. 40 (2015) 155-164

SYNTHESIS OF POROUS SILICON BY ION IMPLANTATION

A.L. Stepanov[1,2,3], V.I. Nuzhdin[1], V.F. Valeev[1], V.V. Vorobev[3], T.S. Kavetskyy[4,5] and Y.N. Osin[3]

[1]Kazan Physical-Technical Institute, Russian Academy of Sciences, 420029 Kazan, Russia
[2]Kazan National Research Technological University, 420015 Kazan, Russia
[3] Interdisciplinary Centre of Analytical Microscopy, Kazan Federal University, 420008 Kazan, Russia
[4]Drohobych Ivan Franko State Pedagogical University, 82100 Drohobych, Ukraine
[5]The John Paul II Catholic University of Lublin, 20-950 Lublin, Poland

Received: July 27, 2015

Abstract. Porous materials have attracted remarkable concerns and found tremendous importance widespread in both fundamental research and industrial applications. Such materials could be widely used for variety applications as absorbents, lightings, catalysts, and for biological molecular filtration and isolation. One quite known method for preparation of porous semiconductor structures is ion implantation, which was successfully used to create porous germanium layers by Ge^+-, Bi^+- and Sn^+-ion irradiation of crystalline germanium substrates. It was also shown that ion implantation suited to produce porous structures in amorphous germanium and SiGe (90% of germanium) alloys thin films. Ion implantation is a well established and all over the world accessible technique, being mainly used for semiconductor microelectronic device fabrication. Unfortunately, a possibility about porous silicon (PSi) fabrication using ion implantation was not completely studied now.

At the present report a novel technological approach based on low-energy ion implantation is suggested and realized to create PSi layers on the crystalline surface of Si wafers. It is demonstrated that using high-dose (more than 1.0×10^{16} ion/cm^2) Ag-ion implantation of silicon with the energy of 30 keV the surface PSi structures with nanoparticles can be successfully fabricated.

1. INTRODUCTION

The remarkable characteristics of nanostructures are typically the result of their nanoscopic dimensions. Forming 3D nano- and microstructured network materials is a way to transfer these special properties to the macroscopic world. Classical semiconductors or ceramics exhibit important fundamental properties including high chemical inertness and high-temperature stability. Porous silicon (PSi) is one of the most widely studied modern structured materials whose application in micro, nano, and optoelectronics, as well as in sensorics, biosensorics, and solar cells, is very promising [1]. Such PSi layer was obtained at first in the mid-1950s at Bell Labs [2], but it was not seriously used until the discovery of its strong luminescent properties in 1990 [3]. Prior to this discovery, PSi was almost exclusively considered as insulating layer devices in the microelectronics industry. The detail advantages of PSi vs. silicon are observed in a literature very well [4,5]. Therefore, searching for new techniques to obtain PSi and improving the corresponding methods, existing for synthesis of such structures, is a topical problem now.

In past, there were only two main technological methods for production of PSi structures: electrochemical etching and chemical stain etching [4,5]. Thus, PSi could be chemically created on silicon under the appropriate conditions with porous sizes

Corresponding author: A.L. Stepanov, e-mail: aanstep@gmail.com

of a few nanometers to micrometers [1,6]. Both the porosity and the pore morphology of PSi are greatly influenced by the electrochemical and chemical stain etching parameters such as temperature, current density, light illumination, and so on.

The method used to obtain nanodimensional PSi layers at the surface of monocrystalline silicon as a result of its implantation with ions of rare gases is also known. The solubility of rare gases in solids is very low and does not exceed a level of 10^{16} ion/cm^2. The gettering of gas bubbles from the matrix gas ions in irradiated polymer material leads to the formation of nanopores (free volumes, nanovoids) [7]. In the case of silicon in order to stimulate the nucleation and growth of pores from implanted gas ions, the implanted silicon wafers are subjected to thermal annealing [8]. Such a technique for the formation of pores at the surface of silicon was demonstrated earlier for implantation with ions such as He^+ [9], H^+ [10], Ne^+ [11], Ar^+ [12] and Kr^+ [11,13].

Additionaly, the interest to silicon nanostructures containing noble metal nanoparticles was recently found. It was initiated because of metal nanoparticles with localized surface plasmon modes demonstrate a specific option to enhance the recombination rate of the light silicon emitter to increase the efficiency of photoluminescence and internal quantum effectively, etc. [6,14-16]. Silver nanoparticles (AgNPs) are the subject of specific increasing interests due to their strongest plasmon resonance in the visible spectrum [17,18]. For example, PSi samples coated with a layer of AgNPs after their electrochemical etching showed that a photoluminescence intensity becomes remarkably increased [19], the reflection of incident light with wavelength below 1100 nm could be reduced to use them for antireflection devices [20] or surface-enhanced Raman scattering of adsorbed on AgNP-PSi structures some organic molecules [15].

Instead of using simple silicon as the substrate for the AgNPs deposition on the top of a sample, the ion implantation technique can be used to form AgNPs in a volume of silicon as in the case of ion-irradiated silica glass or polymers [18,20- 24]. Early, in experiments of the works [25,26] Ag-ion implantation into crystalline silicon wafers and silicon nanocrystal layers at the energy of 30-35 keV and rather lower dose of 5.0×10^{15} ion/cm^2 was performed. Then AgNPs in silicon matrix were synthesized after thermal annealing at 500 °C of implanted samples. In another work [27] Ag^+-ion implantation of silicon using a conventional metal vapor vacuum arc - MEVVA ion source, which produced a mixture

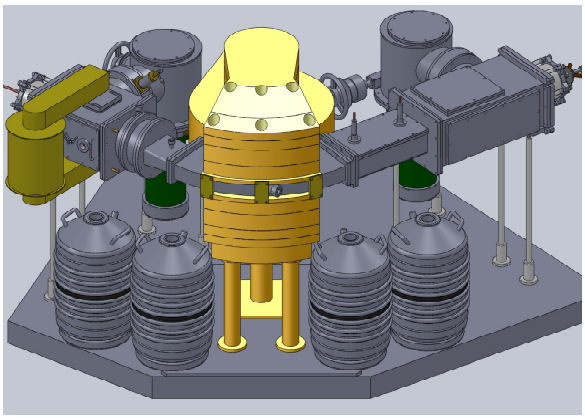

Fig. 1. The ion accelerate ILU-3.

of Ag^{n+} ions, was applied at higher dose of 2.0×10^{17} ion/cm^2 to create AgNPs.

As it will be discussed here and as it was shown in the scientific literature [28], the metal-ion implantation physical technique was not used before 2013 in practice for fabrication of PSi [29]. In the articles [29,30], a first time it was demonstrated a successful experiment on synthesis of PSi with implanted Ag nanoparticles. A detailed description of technological approach and a new result data for AgNP-PSi are demonstrated and explained in this report.

2. EXPERIMENTAL

A *p*-type (100)-oriented single crystalline silicon wafers as the substrate were used for Ag^+-ion implantation to create PSi structures. Before implantation the substrates were cleaned in a wet chemical etching process. The silicon wafers were implanted with Ag^+ ions at an energy of 30 keV and the ion current density of 8 μA/cm^2 with doses in the range between 7.5×10^{16} and 1.5×10^{17} ion/cm^2 using the ion accelerate ILU-3 (Fig. 1) at residual vacuum of 10^{-5} Torr and room temperature of the irradiated samples.

In an additional experiment, in order to reveal an effect of sputtering or swelling of the surface, some silicon substrates were implanted through a mask consisting of a mesh nickel grid with square holes and the bar width of 20 μm. The mask was imposed onto the substrate during implantation to form a step between irradiated and non-irradiated parts of the silicon surface. In this way, selectively implanted regions next to unimplanted ones were prepared in order to perform the step-height profilimetry.

Depth distribution profiles of Ag atoms and the damage level in implanted silicon were modeled using the simulation-program the Stopping and Range of Ions in Matter (SRIM-2013) [31]. The morphology of the implanted structured silicon sur-

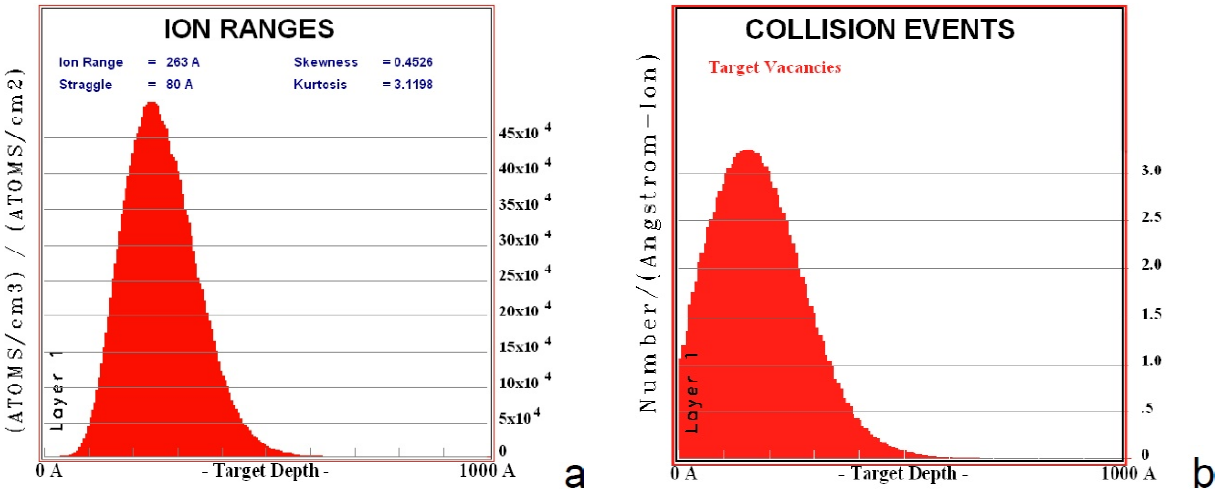

Fig. 2. Depth ion distribution of Ag-ions implanted (a) and generated vacancy profiles (b) in silicon with energy of 30 keV calculated using the SRIM code.

faces were characterized in plane-view by scanning electron microscopy (SEM) using high-resolution microscope Merlin Carl Zeiss combined with ASB (Angle Selective Backscattering) and SE InLens (Secondary Electrons in lens direction) detectors, which was also equipped for energy-dispersive X-ray spectroscopy (EDX) analysis with AZTEC X-MAX energy-dispersion spectrometer from Oxford Instruments. The crystallinity of the implanted silicon structure was estimated by the spectra of Raman scattering (RS) registered on a DFS-52 spectrometer at room temperature and excited by a continuous argon laser LGN-502 at a wavelength of 448 nm and radiation power of 50 mW. Surface morphology observation and the measurements of the profile and depth of pores (cross section) in PSi were carried out also by an Innova Bruker atomic-force microscope (AFM). A quantitative evaluation of the size of pores was carried out by histograms with the size distribution using Axio Vision computer software for processing SEM images according to the method described in the work [32]. Focusing ion beam (FIB) technique was applied to provide a milling of implanted silicon surface for analyzing a sample depth by Auriga CrossBeam Workstation Carl Ziess (FIB-SEM) with 30 KeV Ga liquid metal ion source at normal incidence. By this approach square of 2 × 2 μm^2 on a PSi surface was written at ion current density of 50 nA/cm^2 that did not heat a sample but effectively sputtered a implanted surface.

3. RESULTS AND DISCUSSION

Ion implantation is a widely applied technique used for the controlled matrix depth doping of various metals, dielectrics, and semiconductors by embedding into them energetically accelerated ions of various chemical elements [1]. According to the SRIM simulations, during ion bombardment an excess vacancy-rich region and accumulation of implanted ions can be formed close to the surface in irradiated matrix (Fig. 2). A mean penetration range (R_p^{Ag}) of 30 keV accelerated Ag^+-ions into silicon substrate is about 26 nm with a longitudinal straggling (ΔR_p^{Ag}) of 8 nm in the Gaussian depth distribution (Fig. 2a). Thus, the assumed predicted thickness of the modified silicon surface layer ($R_p + 2\Delta R_p$) is about 42 nm.

It was assumed [33] that during ion implantation porous structures in various semiconductors could be resulted from nucleation of small voids in the irradiated materials by vacancy generations. Therefore the vacancy depth distribution for silicon implanted with Ag^+ ions was also simulated by the SRIM (Fig. 2b), which showed similar profile to ion distribution for such low accelerating energies. Analyzing SRIM modeling, however it should be taking in account that obtained depth distribution of silver and vacancies are corresponded to implantation process of uniform silicon matrix before a nucleation and growth (for ion dose less then 1.0×10^{16} ion/cm^2) of PSi. As it will be shown further, a prolonged irradiation, simultaneously with the formation of PSi and a segregation of silver near the surface, results in silicon sputtering.

Fig. 3a shows a plane-view SEM image of unimplanted silicon, which looks likes as very smooth without any surface structural inhomogeneity. The results of porosification of the silicon samples are observed by plan-view SEM images (Fig. 4). In contrast to unimplanted silicon (Fig. 3) the characteristic PSi surface structures show the

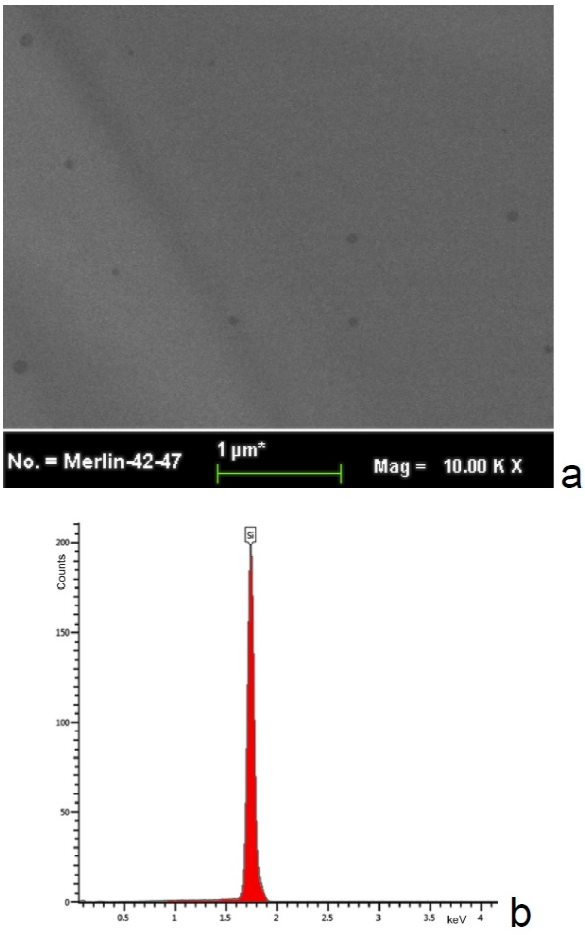

Fig. 3. SEM image (a) and EDX characteristic spectrum (b) of unimplanted silicon.

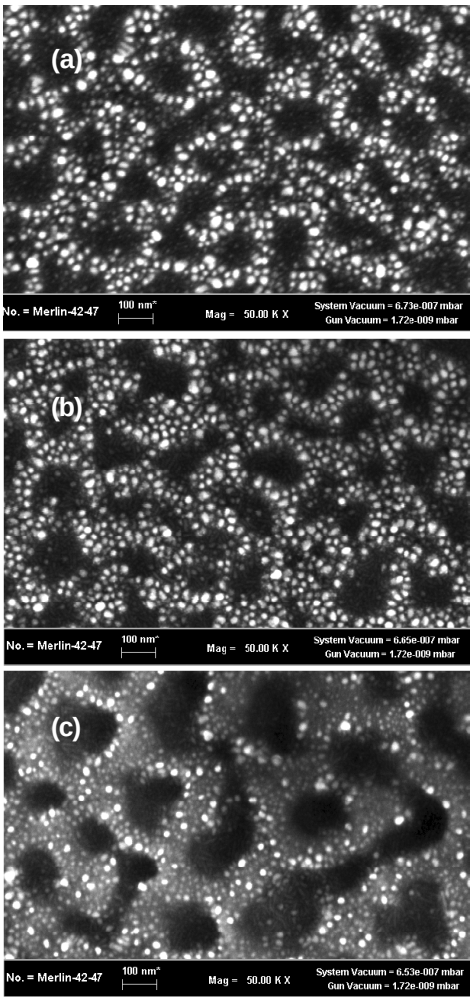

Fig. 4. SEM images of PSi fabricated by Ag^+-ion implantation of silicon at various doses: (a) 7.5×10^{16}; (b) 1.0×10^{17} and (c) 1.5×10^{17} ion/cm^2.

black hole appearance in the implanted silicon region. They are consisting of near cellular features partitioned by rather thin walls with thicknesses about 30-60 nm. Such features are clearly resolved in all samples formed by various Ag-ion dose irradiations: 7.5×10^{16}, 1.0×10^{17}, and 1.5×10^{17} ion/cm^2. Uniform pore distributions with distinguished sharp holes over all implanted surfaces on implanted silicon samples were observed. The size of pores were measured by counting the number of holes in several micrographs, taking into account all visible holes boundaries and subtracting those holes that intersects an edge of the SEM image. From this, the size of the pores was estimated. It is seen that mean size of pores (black holes) increasing in magnitude with an increasing of Ag-ion doses. A white spots in these SEM figures correspond to material with higher density against to silicon that suggests them to be AgNPs.

It is shown in Fig. 3b and Fig. 5, EDX spectra recorded on the examined unimplanted silicon and PSi structures with AgNPs fabricated at highest ion dose, respectively. Such EDX spectra measurements for implanted samples were done in the area on surface outside black holes of the silicon pores. In contrast to EDX data for unimplanted silicon, in the middle part of the presented spectra of PSi it is clear seen four peaks located between 2.5 and 3.5 keV.

Those maxima are directly related to the Ag characteristic lines. It is observed that the intensity of Ag EDX peaks increases with increasing of ion implantation dose that means a growing of Ag concentrations in the silicon samples. Appearance of Ag peaks is in consistence with white sports in SEM images of the PSi (Fig. 4), which are corresponding to AgNPs synthesized in PSi during ion implantation. As shown in the present study, using selected conditions for low-energy Ag-ion irradiation of silicon AgNPs can be fabricated without post-implantation thermal annealing as it was applied in the works [25,26].

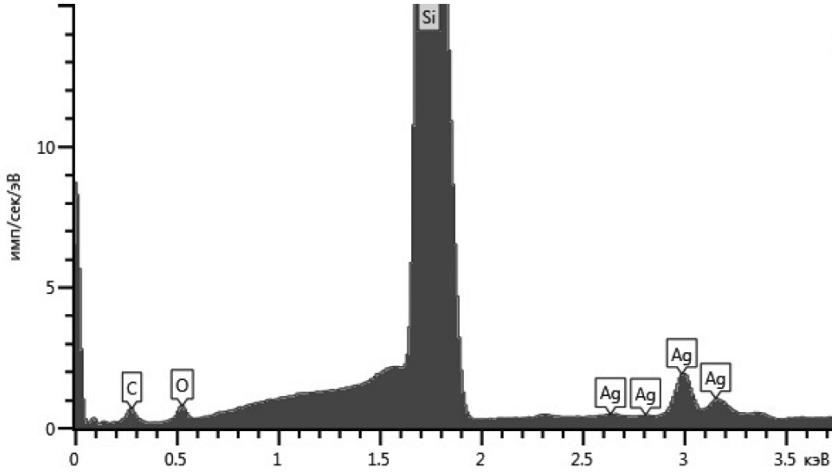

Fig. 5. EDX characteristic spectrum of PSi fabricated at ion dose of 1.5×10^{17} ion/cm^2. Visible EDX peaks confirm the presence of Ag in the synthesized PSi structures.

For the applied FIB conditions of PSi treatment, the mean penetration depth of Ga^+-ions implanted into silicon was obtained by SRIM calculation, which gives a value R_p^{Ga} = 28 nm with a straggling (ΔR_p^{Ga}) of 10 nm in the Gaussian depth distribution. Fig. 6 represents a SEM image of a FIB-milled cross-section of an irradiated area of the surface with PSi from Fig. 4c. The whole thickness of the affected layer is about 1 μm. On the walls of a recess a more or less closed short columnar structure (shown by arrows) with approximately size of several tens nanometers could be recognized, which expends from the surface to the depth of the sample.

Fig. 7 shows SEM images in various scales of the silicon surface implanted with silver ions. Opposite to the initial polished substrate, the morphol-

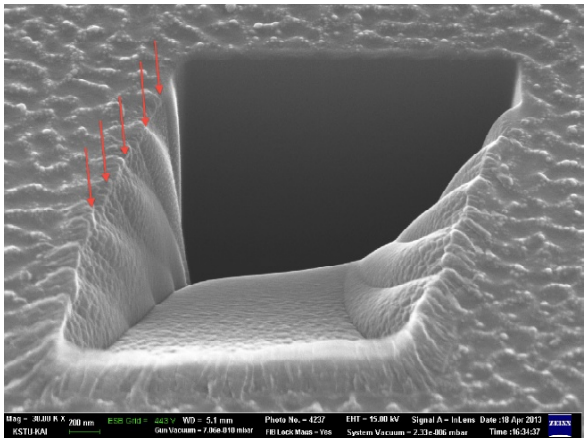

Fig. 6. SEM image of sample surface with PSi structures (as in Fig. 4a) fabricated at an Ag^+-ion dose of 1.5×10^{17} ion/cm^2 after FIB treatment with Ga ions. Arrows show top positions of vertically continued porous on the wall of a recess in the FIB-milled cross-section.

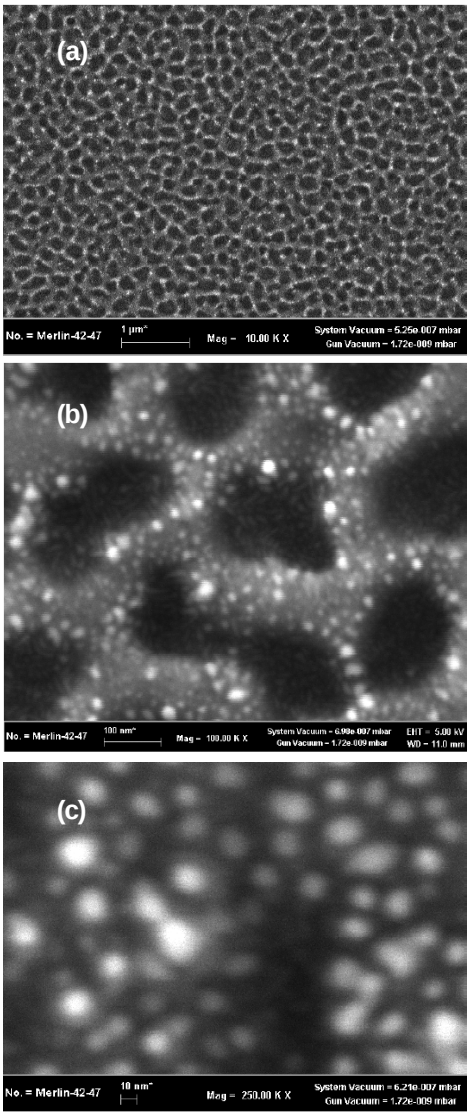

Fig. 7. SEM images of PSi structure fabricated at a dose of 1.5×10^{17} ion/cm^2 presented with different scales: (a) 1 μm; (b) 100 nm; (c) 10 nm.

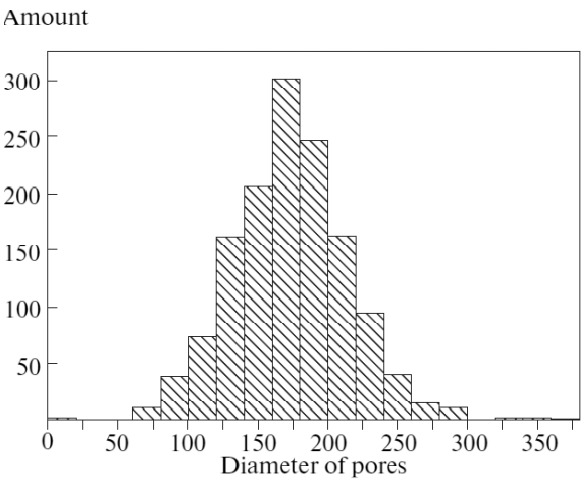

Fig. 8. Histogram of pore size distribution in a structure of PSi (Fig. 7b) formed by implantation of silicon with silver ions.

ogy of the irradiated silicon surface is caused by the typical PSi structure. As can be seen from Fig. 7a, the layer of PSi formed by implantation looks very homogeneous on a rather large area of the sample (of tens of microns), which is topical for a number of technological applications (scaling). The increase in a surface fragment (Fig. 7b) allows estimating the average diameter of pore holes (black blemishes) amounted to about 150–180 nm, as follows from the histogram of pore size distribution (Fig. 8). The thickness of pore walls is estimated to be of a value on the order of 30–60 nm. A further increase in the scale (Fig. 7c) indicates the formation of synthesized implantation nanoinclusion (light blemishes) in the structure of PSi walls with an average size on the order of 5–10 nm. Since heavier chemical elements registered by the detector of backscattered electrons are revealed in SEM microphotographs in a lighter tone then for a composite material composed of silicon atoms alone and implanted silver, it is possible to conclude that light (white) regions observed on a dark background (signal from silicon) are determined by the formed metal silver in the form of nanoparticles (Fig. 7c). In this case it could be noted that silver atoms do not form any chemical compounds with silicon, similar to silicide of metals (cobalt, iron, etc.).

It follows from the measurements of optical Raman scattering spectra for irradiated and nonirradiated silicon that the peak registered at a frequency of 520 cm^{-1}, associated, as it is known [34], with scattering on optical phonons of the crys-

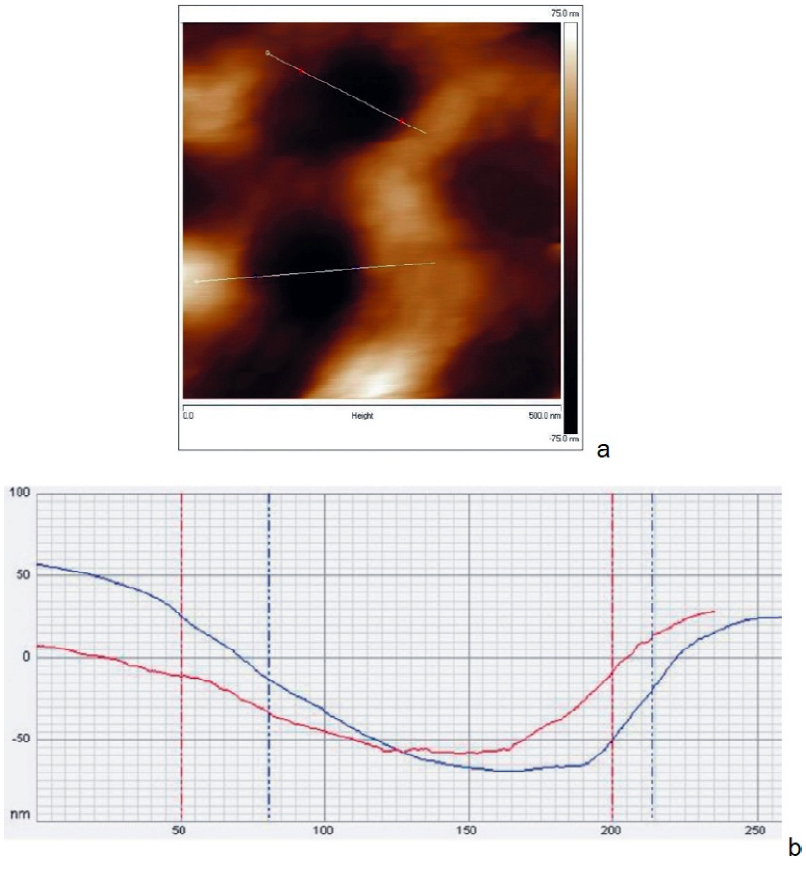

Fig. 9. (a) AFM images of the PSi surface obtained by silicon implantation with Ag ions and (b) profiles of individual pores measured on the directions shown in figure (a).

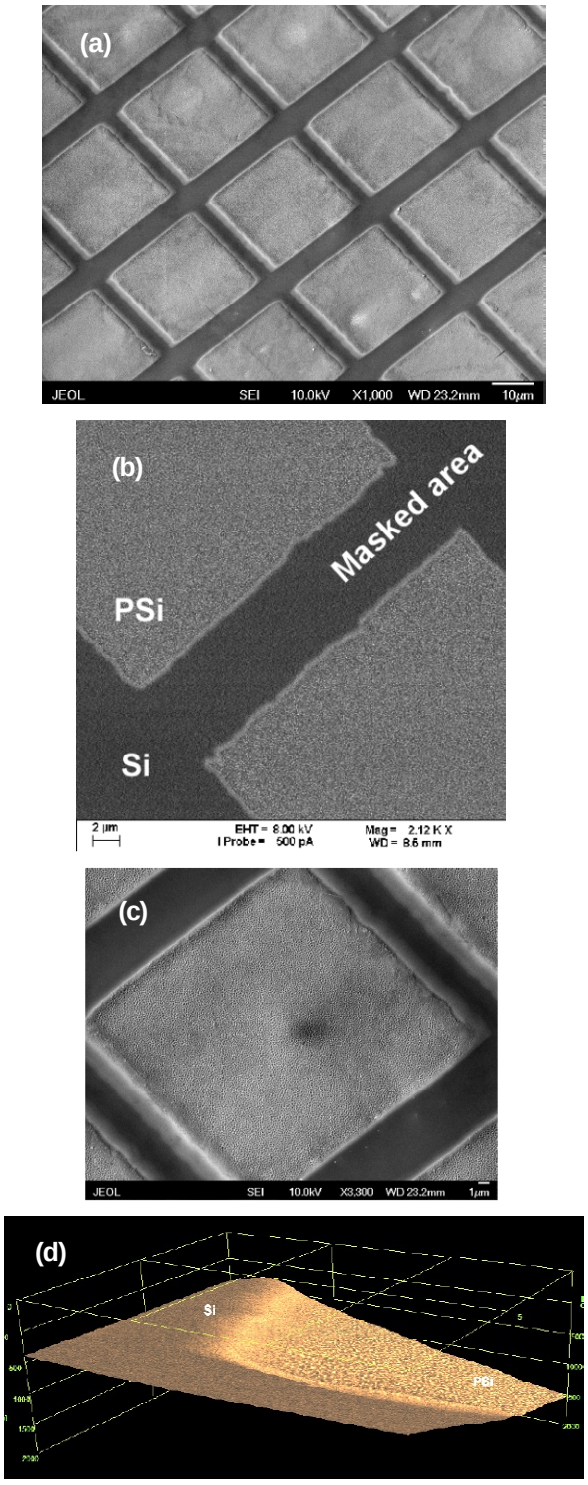

Fig. 10. (a), (b) (c) SEM images (different scales) of structures with PSi (light gray) fabricated at a Ag^+-ion dose of 1.5×10^{17} ion/cm^2 through a mesh nickel mask. (d) 3D SEM reconstruction of step area that demonstrates a sputtering of the silicon surface during Ag-ion implantation.

talline silicon matrix, disappears completely after ion implantation, which characterizes the formed PSi layer as amorphous.

Additional information proving the formation of PSi by silicon implantation with Ag ions is obtained by AFM measurements. Fig. 9a presents the AFM image, which was observed as a fragment of the PSi surface, looking typical for porous structures in the case of AFM measurements [13]. Fig. 9b shows the profiles of cross sections of individual pores measured on the directions shown in Fig. 9a, allowing estimating of the depth of pores amounting to a value on the order of 100 nm. Thus, it can be concluded that, as a result of silicon implantation with silver ions, characteristic pores are formed comparable with relatively shallow pores in PSi obtained by an electrochemical method in highly diluted solutions of hydrofluoric acid [4].

In order to estimate the formed step at the interface between the irradiated and non-irradiated regions of silicon by swelling the surface or its sputtering during ion implantation, in particular, by the formation of pores in semiconductors, for instance, in germanium by an irradiation with an ion of germanium, implantation through a mask is commonly suggested [28]. SEM image of a silicon surface containing fragments of PSi microstructures formed in this work by implantation with silver ions with a dose of 1.5×10^{17} ion/cm^2 through a mask is shown in Fig. 10. As can be seen from the step-height data (Figs. 10a - 10c), rectangular PSi light-gray regions were formed at the surface of silicon as a result of implantation, which were confined by dark strips of non-irradiated crystalline silicon. 3D reconstruction part of sample close to edge corner mask presented in Fig. 10d, illustrating the direct evidence for sputtering of Ag^+-ion implanted silicone surface. In first approximation, it could be speculated that the volume expansion is related to a mechanism simply governed by the nuclear energy deposition, which is usually measured in displacement per atom [33].

A fragment of a sample comprising a region of several square bars of the mask given in 3D projections of an AFM image is shown in Fig. 11. As can be also seen from these figures, an efficient sputtering of the silicon-substrate surface takes place during the implantation of silicon with ions of silver and the formation of a porous structure. Earlier, the sputtering and erosion of the silicon surface were observed by its irradiation with accelerated argon ions in an energy range of 50–140 keV [35]. However, there was no information about the formation of pores in this publication. As a result of implantation with Ag ions, a hollow and step are formed at the interface between silicon and PSi of the irradiated part of silicon.

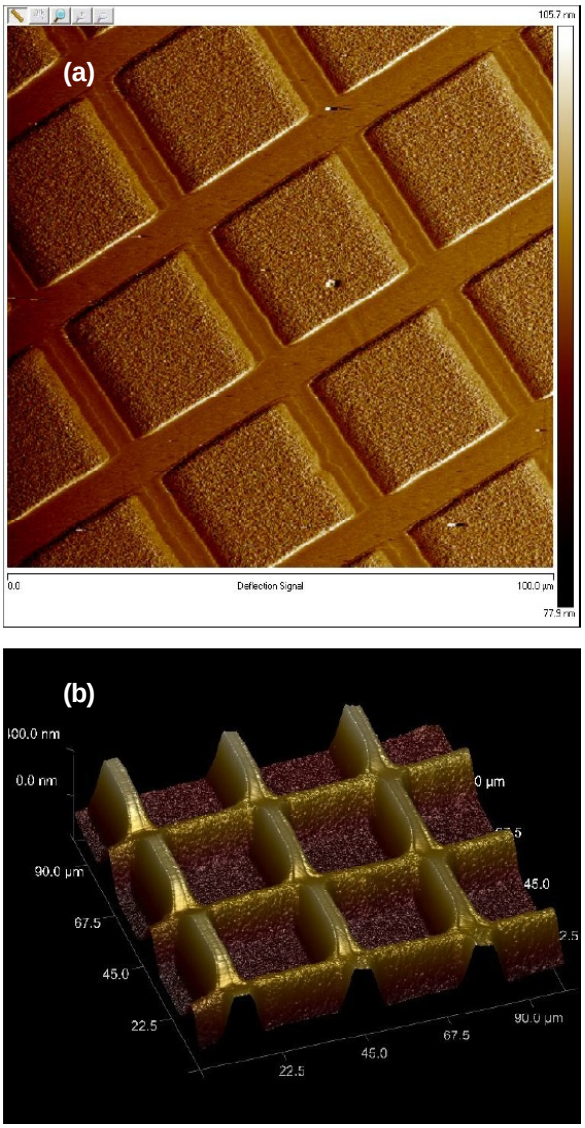

Fig. 11. (a) and (b) 3D fragment of an AFM image of the surface in the mask region, which demonstrates sputtering of silicon.

It is known that for a critical rather-low implantation dose, silicon undergoes a crystalline to amorphous phase transition [36,37]. As seen from the results reported in this work at higher doses, the amorphous silicon layer transforms to a porous structure with AgNPs. Thus, for the first time in practice, it is demonstrated by present experiment that PSi growth was stimulated by high-dose metal-ion implantation. This new result for silicon could be considered in consistence with published data for porous semiconductors, in particular, for germanium fabricated during ion implantation process [28,38-40] and a similar suited possible mechanism for PSi structuring could also be considered. The spattering effect (Figs. 9 and 10) seems to be important for determining the mechanism of PSi formation, and it appears somewhat unexpected, since it is known that, by the formation of pores in implanted semiconductors (germanium), an opposite phenomenon was observed: the swelling of the surface [28]. Therefore, the proposed mechanism of pore formation in implanted germanium based on the generation of vacancies in an irradiated semiconductor, which join the pores, cannot be merely transferred to the matrix of Si implanted with ions of silver. Despite PSi creation by metal-ion implantation of silicon, in the case of germanium over the past 30 years there was much debate regarding mechanism governed a formation of the porous semiconductor structure in ion-implanted germanium [41]. Currently, there are two main theories of void formation for germanium: vacancy clustering and so-called **"**microexplosions**"**. The vacancy clustering theory invokes the inefficient recombination of germanium point defects during ion implantation, where once a critical point defect population is created by ion implantation, excess vacancies cluster into pores in order to minimize the dangling bond density. In contrast, the microexplosion theory is based on the creation of voids through pressure waves and thermal spikes caused by the overlap of ion cascades [41]. Therefore, in principle, it is possible to determine which theory better models void and porous formation in silicon by selecting appropriate implant conditions and observing the resulting microstructure after implantation.

4. CONCLUSIONS

Thus, in this work a completely new technique used to obtain PSi layers with silver nanoparticles at the surface of monocrystalline silicon by a low-energy high-dose implantation was demonstrated. Ion implantation is one of the basic techniques used in industrial semiconductor microelectronics for the formation of various types of silicon nano- and microdevices. Therefore, the proposed new physical technique for the formation of PSi, in contrast to the well-known chemical approaches, rather easily integrated into an industrial modern process for improving the technologies of the fabrication of microcircuits.

As follows from the results presented in this work, in our experiments the PSi structures with silver nanoparticles were first obtained without a chemical technique in solution. Evidently, the further steps in improving such types of composite materials must contain an optimization of the processes of their fabrication and, in particular, searching for correlation features between structural parameters and the characteristics of optical, plas-

mon, photoluminescence, and sensor properties of new porous structures.

ACKNOWLEDGEMENTS

T.S. Kavetskyy acknowledges the SAIA (Slovak Academic Information Agency) for scholarships in the IPSAS within the National Scholarship Program of the Slovak Republic. A.L. Stepanov thanks for the financial support by the Russian Scientific Foundation (No. 14-13-00758). This work was also partly supported by the Russian Foundation for Basic Research (Nos. 12-02-00528 and 13-02-12012) and by the State Fund for Fundamental Researches of Ukraine (No. F52.2/003). Authors are grateful to A. Denisov for help with SEM measurements.

REFERENCES

[1] V. Torres-Costa and R.J. Martin-Palma // *J. Mater. Sci.* **45** (2010) 2823.
[2] A. Uglir // *Bell Syst. Tech. J.* **35** (1956) 333.
[3] L.T. Canham // *Appl. Phys. Lett.* **57** (1990) 1046.
[4] Z.C. Feng and R. Tsu, *Porous silicon* (World Sci. Publ., New York, 1994).
[5] M.J. Sallor, *Porous silicon in practice* (Willey-VCH, Weinheim, 2011).
[6] G. Oskam, J.G. Long, A. Natarajan and P.C. Searson // *J. Phys. D: Appl. Phys.* **31** (1998) 1927.
[7] T. Kavetskyy, V. Tsmots, A. Kinomura, Y. Kobayashi, R. Suzuki, H.F.M. Mohamed, O. Sausa, V. Nuzhdin, V. Valeev and A.L. Stepanov // *J. Phys. Chem. B* **118** (2014) 4194.
[8] V.V. Kozlovskii, V.A. Kozlov and V.N. Lomasov // *Semiconductors* **34** (2000) 123.
[9] H.J. Stein, S.M. Myers and D.M. Follstaedt // *J. Appl. Phys.* **73** (1993) 2755.
[10] G.F. Cerofolini, L. Meda, R. Balboni, F. Corni, S. Frabboni, G. Ottaviani, R. Tonini, M. Anderle and R. Canteri // *Phys. Rev. B* **46** (1992) 2061.
[11] M. Wittmer, J. Roth, P. Revesz and J.M. Mayer // *J. Appl. Phys*. **49** (1978) 5207.
[12] P. Revesz, M. Wittmer, J. Roth and J.M. Mayer // *J. Appl. Phys.* **49** (1978) 5199.
[13] M.F. Galyautdinov, N.V. Kurbatova, E.Y. Buinova, E.I. Shtyrkov and A.A. Bukharaev // *Semiconductors* **31** (1997) 970.
[14] T.S. Amran, M.R. Hashim, N.K. Al-Obaidi, H. Yazid and R. Adnan // *Nanoscale Research Lett.* **8** (2013) 35.
[15] S. Chan, S. Kwon, T.-W. Koo, L.P. Lee and A.A. Berlin // *Adv. Mat.* **15** (2003) 1595.
[16] M.Wang, X. Wang and S. Ghoshal // *Micro & Nano Lett.* **8** (2013) 465.
[17] U. Kreibig and M. Vollmer, *Optical Properties of Metal Clusters* (Springer, Berlin, 1995).
[18] A.L. Stepanov, *Ion-synthesis of silver nanoparticles and their optical properties* (Nova Sci. Publ., New York, 2010).
[19] D.T. Cao, L.T.Q. Ngan and C.T. Anh // *Surf. Interface Anal.* **45** (2013) 762.
[20] Y. Wang, Y.P. Liu, H.L. Liang, Z.X. Mei and X.L. Du // *Phys. Chem. Chem. Phys*. **15** (2013) 2345.
[21] R.A. Ganeev, A.I. Ryasnyansky, A.L. Stepanov and T. Usmanov // *Phys. Stat. Sol. B* **241** (2004) R1.
[22] A.L. Stepanov, S.N. Abdullin, V.Y. Petukhov, Y.N. Osin and I.B. Khaibullin // *Phil. Mag. B* **80** (2000) 23.
[23] A.L. Stepanov and V.N. Popok // *Surf. Sci.* **566** (2004) 1250.
[24] A.L. Stepanov // *Rev. Adv. Mater. Sci.* **26** (2010) 1.
[25] A.K. Sing, K.G. Gryczynski, F.D. McDaniel, S.Y. Park, M. Kim and A. Neogi // *Appl. Phys. Express* **3** (2010) 102201.
[26] A.K. Sing, K.G. Gryczynski and A. Neogi // *Opt. Mater. Express* **2** (2012) 501.
[27] H.W. Seo, Q.Y. Chen, I.A. Rusakova, Z.H. Zhang, D. Wijesundera, S.W. Yeh, X.M. Wang, L.W. Tu, N.J. Ho, Y.G. Wu, H.X. Zhang and W.K. Chu // *Nucl. Instr. Meth. Phys. Res. B* **292** (2012) 50.
[28] L. Romano, G. Impellizzeri, M.V. Tomasello, F. Giannazzo, C. Spinella and M.G. Grimaldi // *J. Appl. Phys.* **107** (2010) 84310.
[29] A.L. Stepanov, A.A. Trifonov, Y.N. Osin, V.F. Valeev and V.I. Nuzhdin // *Optoelecton. Adv. Mater. - Rapid Commun.* **7** (2013) 692.
[30] A.L. Stepanov, Y.N. Osin, A.A. Trifonov, V.F. Valeev and V.I. Nuzhdin // *Nanotechnologies in Russia* **9** (2014) 163.
[31] J.F. Ziegler, J.P. Biersack and U. Littmark, *The stopping and range of ions in solids* (Pergamon Press, New York, 1985), http://www.srim.org/.
[32] J. Peckham and G.T. Andrews // *Semicond. Sci. Technol.* **28** (2013) 105027.
[33] L.M. Wang and R.C. Birtcher // *Appl. Phys. Lett*. **55** (1989) 2494.
[34] I.E. Tyschenko, V.P. Popov, A.B. Talochkin, A.K. Gutakovskii and K.S. Zhuravlev // *Semiconductors* **38** (2004) 107.

[35] T.K. Chini, M.K. Sanyal and S.R. Bhattacharyya // *Phys. Rev. B* **66** (2002) 153404.
[36] E. Chason, S.T. Picraux, J.M. Poate, J.O. Borland, M.I. Current, T. Diaz de la Rubia, D.J. Eaglesham, O.W. Holland, M.E. Law, C.W. Mayer, J. Melngails and A.F. Tasch // *J. Appl. Phys.* **81** (1997) 6513.
[37] J.S. Williams // *Mater. Sci. Eng. A* **253** (1998) 8.
[38] L. Romano, G. Impellizzeri, L. Bosco, F. Ruffino, M. Miritello and G. Grimaldi // *J. Appl. Phys.* **111** (2012) 113515.
[39] T.M. Donovan and K. Heinemann // *Phys. Rev. Lett.* **27** (1971) 1794.
[40] T. Steinbach, J. Wemecke, P. Kluth, M.C. Ridgway and W. Wesch // *Phys. Rev. B* **35** (1987) 104108.
[41] B.L. Darby, B.R. Yates, N.G. Rudawski, K.S. Jones, A. Kontand and R.G. Elliman // *Thin Solid Films* **519** (2011) 5962.